

## Video Article

# Planar Gradient Diffusion System to Investigate Chemotaxis in a 3D Collagen Matrix

David A. Stout<sup>1</sup>, Jennet Toyjanova<sup>2</sup>, Christian Franck<sup>3</sup><sup>1</sup>Department of Mechanical and Aerospace Engineering, California State University, Long Beach<sup>2</sup>Ximedica<sup>3</sup>School of Engineering, Brown UniversityCorrespondence to: David A. Stout at [david.stout@csulb.edu](mailto:david.stout@csulb.edu)URL: <http://www.jove.com/video/52948>DOI: [doi:10.3791/52948](https://doi.org/10.3791/52948)

Keywords: Bioengineering, Issue 100, Chemotaxis, 3D cell migration, diffusion, traction force microscopy, gradient, live-cell imaging

Date Published: 6/12/2015

Citation: Stout, D.A., Toyjanova, J., Franck, C. Planar Gradient Diffusion System to Investigate Chemotaxis in a 3D Collagen Matrix. *J. Vis. Exp.* (100), e52948, doi:10.3791/52948 (2015).

## Abstract

The importance of cell migration can be seen through the development of human life. When cells migrate, they generate forces and transfer these forces to their surrounding area, leading to cell movement and migration. In order to understand the mechanisms that can alter and/or affect cell migration, one can study these forces. In theory, understanding the fundamental mechanisms and forces underlying cell migration holds the promise of effective approaches for treating diseases and promoting cellular transplantation. Unfortunately, modern chemotaxis chambers that have been developed are usually restricted to two dimensions (2D) and have complex diffusion gradients that make the experiment difficult to interpret. To this end, we have developed, and describe in this paper, a direct-viewing chamber for chemotaxis studies, which allows one to overcome modern chemotaxis chamber obstacles able to measure cell forces and specific concentration within the chamber in a 3D environment to study cell 3D migration. More compelling, this approach allows one to successfully model diffusion through 3D collagen matrices and calculate the coefficient of diffusion of a chemoattractant through multiple different concentrations of collagen, while keeping the system simple and user friendly for traction force microscopy (TFM) and digital volume correlation (DVC) analysis.

## Video Link

The video component of this article can be found at <http://www.jove.com/video/52948/>

## Introduction

The preferred movement of cells towards a concentration gradient, known as chemotaxis, plays an important role in pathological and physiological processes in the body. Such examples are skin and mucosa wound healing<sup>1</sup>, morphogenesis<sup>2</sup>, inflammation<sup>3</sup>, and tumor growth<sup>4,5</sup>. It has also been shown that cancer cells can migrate through both individual and collective cell-migration strategies<sup>6</sup>. Moreover, diffusional instability mechanisms can induce the separation of single or clustered cells from a tumorous body/object and then can immigrate towards a source of nutrients and thus invade wider areas and tissues<sup>7</sup>.

Furthermore, it has been shown that diverse migration mechanisms can be active in 2D and in 3D, due to different roles of adhesion molecules<sup>8</sup>. Therefore, a move to physiologically relevant *in vitro* assays to investigate cell motility in a measurable and simple way is of significance in understanding cell movement phenomena<sup>9</sup>. Unfortunately, the difficulty in analyzing cell migration, a comprehensive quantifiable chemotaxis assay usually requires a long laborious method, founded on the measurement of impartial cell motility and transport phenomena models.

Past experimental approaches to investigate cell chemotaxis include the Boyden chamber<sup>10</sup> and the under agarose assay<sup>11</sup>. However, within these early assays, cell migration experiments did not monitor the movement in respect to time. More, importantly, the concentration gradients used for the experiments were not well defined or completely understood while only sustaining the signaling for no more than a few hr. Furthermore, early chemotaxis chamber attempts restricted cell migration to two dimensions and did not allow one to monitor the kinetics of migration<sup>12</sup>. Looking at the Boyden chamber, an endpoint assay would not allow the researcher to observe migration visually and could not directly differentiate chemotaxis (directional movement) from chemokinesis (random movement). Additionally, several variables—differences in the pore size and thickness of membranes—made the chamber very difficult to easily reproduce and concealed the migrant reaction of cells to chemokines<sup>13,14</sup>.

With the new understanding of microfluidics, new chambers and micro-devices have been investigated as an instrument to investigate cell locomotion under interstitial flow conditions or chemotaxis<sup>15,16</sup>. Under these new devices, new cell metrics were introduced and investigated, like the effect of shear stress on a cell<sup>17,18</sup>. Unfortunately, past and current microfluidic chemotaxis chambers limited studies of cell migration to 2D substrates—an important setback since many biological processes, including tumor cell invasion and metastasis, and immune cell migration, involve 3D migration.

Direct observation chambers—where a chemoattractant solution is in contact with a 3D gel containing cells have also been reported<sup>19,20</sup>. These chambers have two compartments, one containing a chemoattractant and one containing cells, are joined beside one another horizontally<sup>21</sup> or as concentric rings<sup>22</sup>. These systems are pointed in the right direction, but do not keep a chemotaxis system for an extended period of time.

Furthermore, researchers have also examined diffusivity through collagen membranes in dialysis cells, as well as the diffusion of tracer molecules through collagen samples subjected to hydrostatic pressure<sup>23-25</sup>. Some diffusion experiments in collagen gels rely on physical and chemical modifications of the gel using magnetic fields and chemical incorporation<sup>26</sup>. A popular method for modeling diffusivity in collagenous tissues relies on the fluorescence imaging of continuous point photobleaching. This method has revealed anisotropy in the diffusion coefficients of macromolecules in oriented collagenous tissues. Yet, photobleaching has been used in articular cartilage and not collagen matrices. While similar, the necessary modeling experiments must be carried through specifically understanding the diffusion coefficient of collagen gels. More importantly, the systems do not utilize a method for measuring cell force generation.

Unfortunately, most systems seem to be missing one or two key elements for an ideal system: the allowing of cell tracking, a diffusion gradient understanding with a chemotactic factor through the matrix, a relatively simple set up with an ease of reproducibility, the minimization of cell-cell interactions, and the ability to measure dimensional units for quantification (*i.e.*, velocity, force, specific concentration). Moghe *et al.*<sup>27</sup> proposed a system that fulfilled most of these requirements in which cells were initially dispersed throughout the gel rather than concentrated on the filter surface, but was difficult to measure forces that the cell generates.

To this purpose, we present a planar gradient diffusion system to investigate chemotaxis in a 3D collagen matrix, which allows one to overcome modern diffusion chamber limitations of existing assays, which is based on time-lapse microscopy, coupled with image analysis techniques to measure cell forces in a 3D environment. This protocol provides a simple, yet innovative way of creating a simple 3D diffusion chamber that can be used to investigate 3D chemotaxis in different cells.

## Protocol

### 1. 3D Mold Design and Parts

#### 1. Mold

- Before working, obtain a silicone elastomer kit, a live cell imaging chamber, a 22 mm glass coverslip, and a machined aluminum metal cube with dimensions 10.07 mm x 3.95 mm x 5.99 mm. Prepare the live cell imaging chamber for molding by placing the coverslip in the bottom holder and assembling the rest of the chamber as directed by the vendor.
- Next, using forceps, place the machined aluminum metal cube in the middle of the live cell imaging chamber housing and on top of the coverslip, and then set aside.
- Mix silicone elastomer solutions according to manufacturer's protocol to make 5 ml of elastomer.
- Using a disposable lab spatula, pour silicone elastomer solution into live cell imaging chamber setup and ensure not to move placed machined aluminum metal cube. Place the system on the lab bench, in a safe location O/N for curing.
- The next morning, deconstruct the live cell imaging chamber, as recommended by the manufacturer and pull out mold using forceps. Using forceps, carefully extract the machined aluminum metal cube from mold. Go to the sink and rinse the mold with deionized water. Place the mold on a paper towel to dry.
- Once dry, using a hobby utility knife, cut slits through the mold, spaced 2.34 mm apart from each longitudinal end, inside the silicone mold. Ensure the mold stays in a safe and dry place until you are ready to construct the system for an experiment.

#### 2. Hydrophilic and Hydrophobic Glass Coverslips Preparation

- To allow the collagen matrix to adhere to a surface, create hydrophilic coverslips:
  - Using a disposable pipette, measure out 150  $\mu$ l of 3-aminopropyl-trimethoxysilane and pour solution in a 50 ml tube. Add 30 ml of 100% ethanol to the 50 ml tube with a second disposable pipette and close the lid. Vortex the solution for 2 min, ensuring complete mixing. Pour solution in a glass Petri dish and set aside.
  - Pour 15 ml of 100% ethyl alcohol in a second Petri dish and set aside (make sure to label dishes).
  - Using a new disposable pipette, measure out 30 ml of deionized water and pour solution into a 50 ml tube. Next, using a new disposable pipette measure out 1,875  $\mu$ l of glutaraldehyde and pour solution into the same 50 ml tube and close the lid. Vortex the solution for 2 min, ensuring complete mixing. Pour mixture into third Petri dish, and set aside.
  - Using forceps, take out one 22 mm round glass coverslip and rinse both sides with 100% ethanol mixture using a disposable pipette.
  - Place rinsed glass coverslip into 3-aminopropyl-trimethoxysilane with 30 ml of 100% ethanol solution dish and allow to sit in solution for 5 min.
  - With forceps, take out glass coverslip and rinse again with 100% ethanol solution with disposable pipette.
  - Drop rinsed glass coverslip into 1,875  $\mu$ l of glutaraldehyde and 30 ml of deionized water mixture and set aside for 30 min.
  - After 30 min, remove glass coverslip with forceps and rinse with deionized water and place onto dry tissue O/N to dry at RT.
  - Repeat coverslip dipping and moving for as many coverslips as needed with the same generated solutions.
- Make hydrophobic coverslips by the given protocol.
  - Add 500  $\mu$ l of tridecafluoro-1,1,2,2-tetrahydrooctyl, 100  $\mu$ l of acetic acid and 19.4 ml of hexane in a 50 ml tube and vortex for 2 min. Pour solution in glass Petri dish and set aside.
  - Using clean forceps, take out one glass coverslip and drop into prepared mixed solution for 2 min. After 2 min have passed, take out glass coverslip with forceps and rinse with deionized water using a disposable pipette and place coverslip onto dry tissue O/N to dry at RT. Store coverslip in plastic Petri dishes until used.

3. Repeat coverslip dipping and moving for as many coverslips as needed with the same generated solutions.

## 2. Mold Assembly

1. Before using molds, using a disposable pipette rinse the mold with 90% ethyl alcohol over a chemical waste container. Next, place the mold in a Petri dish filled with deionized water and allow to sit O/N.
2. Take mold out of solution using forceps and place on a towel to air dry before starting the mold assembly.
3. While the mold is air-drying, cut the square hydrophilic coverslips into two rectangles slightly larger than 3.95 mm x 5.99 mm using a high-precision diamond-scribing tool. Slide each cut rectangle coverslip into the slots cut into the silicone mold.
4. Flip the mold upside down and apply vacuum grease along the bottom of the silicone mold using a disposable pipette. Next, flip the mold back right-side up and press the bottom of the mold onto the circular hydrophilic glass coverslip to create a seal.
5. With disposable gloves, pick up the assembled mold and place into a disposable Petri dish and then into a bio-hood. Turn on UV Bio-hood lamp for 1 hr to sterilize the mold before experimentation occurs.

## 3. Collagen Mixture and 3D Matrix

1. Before preparing the collagen mixture, stain and prepare cells for imaging according to standard protocols<sup>28</sup>.
2. Using standard laboratory techniques and protocols<sup>29,30</sup>, in a bio-hood, mix cell media and chemoattractant in a 15 ml tube to desired chemoattractant concentration. Pipette 5 ml of specific cell media-chemoattractant concentration solution into a 15 ml tube and move the solution into a heated water bath.
3. Using a pipette, extract 5 ml of just cell media into a second 15 ml tube and place in a heated water bath to heat up the solution for microscopy experiments.
4. In a bio-hood, pipette 30  $\mu$ l of 10x phosphate buffered solution (PBS) into micro centrifuge tube. Add 6  $\mu$ l of 1 N sodium hydroxide (NaOH) into same micro centrifuge tube and vortex for 15 sec.
5. Obtain collagen I rat tail solution from the fridge and move to the bio-hood using standard laboratory techniques and protocols<sup>29</sup>. Ensure the collagen is still cold. Pipette 168.3  $\mu$ l of collagen into same micro centrifuge tube.
6. Next, add 18  $\mu$ l of yellow-green fluorescent carboxylate-modified microspheres using a pipette to the same micro centrifuge tube. Vortex the micro centrifuge tube with all the solutions for 30 sec.
7. Add 77.7  $\mu$ l of desired cell media-cell mixture (approximately  $2 \times 10^6$  cells/ml concentration) into micro centrifuge tube and mix using pipette tip for 20 sec. As necessary, alter the matrix density by following the custom collagen mixture adapted for the addition of fluorescent beads and cell viability table (**Table 1**).
8. Pipette 300  $\mu$ l of collagen-cell mixture into the center well (well #2) of the prepared mold assembly. Place the mold onto a disposable Petri dish and move it into a standard incubator for 20 min at 37 °C with 5% CO<sub>2</sub>.
9. Remove system from incubator and place back into bio-hood. Using forceps, remove both hydrophobic cover slips by clamping onto the top of each coverslip and pulling up and away from the mold.
10. Move the whole system to the desired microscopy and image to ensure collagen mold sides are still straight to allow for a planar diffusion gradient.
11. With the system still under the microscope, using a 100  $\mu$ l single-channel pipette, add 100  $\mu$ l of cell media into well #1. Next, using a 100  $\mu$ l single-channel pipette add 100  $\mu$ l of cell media with desired chemoattractant concentration into well #3.
12. Immediately after adding solutions into both wells, commence imaging.

## 4. Imaging and Diffusion Modeling

1. If one wants to find the diffusion coefficient for the specific collagen density to calculate the specific concentration, follow the protocol below:
  1. Follow the given protocol above titled "Collagen Mixture and 3D Matrix," instead of generating cell media with desired chemoattractant concentration, make 5  $\mu$ M rhodamine in a 15 ml tube using standard calculations and protocols<sup>30</sup>.
  2. Image the 3D collagen matrices with a confocal system mounted on an inverted microscope using an argon laser (488 nm) to capture the fluorescence. Image every 2 or 3 sec for up to 7 hr.
2. For Diffusion Modeling: Using the mathematical model shown below, write a computational software code for processing and analysis with these general steps.

$$C(x, t) = \left[ C_1 + \frac{x}{L} (C_2 - C_1) \right] + \sum_{n=1}^{\infty} a_n e^{-n^2 \pi^2 \alpha^2 t / L^2} \sin\left(\frac{n\pi x}{L}\right)$$

1. Import images into computational software for rescaling and normalizing by the maximum intensity. Convert images to a gray color-map of the image to select the edge. Pick an axis along the center of the image, to the right of the center and to the left of the center.
2. Using the computational software code, plot the normalized intensity, along with the true intensity and the difference between the two.
3. Next, input the parameters necessary for fitting (concentration, time, and length).
4. Plot the normalized concentration versus time and the concentration profile across the x-axis with a polynomial fit to the data.
5. Calculate the coefficient of diffusion using the computational software code.

## 5. Experimental Measurements

1. Referring back to the diffusion equation, rewrite the equation to find the specific concentration at any location within the system as shown in below.

$$\frac{c(x, t)}{c_{max}} = \frac{x}{L} + \frac{2}{\pi} \sum_{n=1}^{\infty} \frac{1}{n} \cos(n\pi) \sin\left(\frac{n\pi x}{L}\right) \exp\left[\frac{-Dtn^2\pi^2}{L^2}\right]$$

Where:

L = Length of the collagen matrix

x = location under investigation

D = coefficient of diffusion

t = elapsed time

2. During chemotaxis experiments, ensure to record the specific time that the moment chemokine was added to system. Once cell migration movement is found, ensure to record confocal time-lapse recording, and note the specific time and location from edge where imaging occurred.
3. During data analysis, plug the noted elapsed time, location and coefficient of diffusion for the specific cell into the equation to find the normalized specific concentration at any point within the collagen for both diffusion and cell experiments.

## 6. Tracking Cell Migration Utilizing TFM

1. To track cell migration using TFM/DVC techniques follow the protocol below:
  1. After the addition of desired chemoattractant concentration into well #3, start imaging the 3D collagen matrices with a confocal system mounted on an inverted microscope to find a cell to investigate.
  2. Once a moving cell is found, place the cell in the middle of the field of view and utilize a piezoelectric motor (to image in the z-axis), image every 1 or 2 min.
  3. For calculating cell force generation and deformation, generate a computational code to find the displacements of the fluorescence beads following the TFM/DVC protocols<sup>31</sup>.

## Representative Results

The ability of this assay to accurately assess the migration of the cell relies upon a good setup of the system. Therefore, it is critical for make sure to design the diffusion system mold accurately and take great care in placing both hydrophobic and hydrophilic coverslips, as illustrated in **Figure 1**. If the system is properly designed and during the diffusion modeling stage ensuring to find a very good linear starting line, one is able to achieve nice fluoresces images, as depicted in **Figure 2**, for analyzing diffusion of the system.

The key to a successful cell chemotaxis analysis is modeling the diffusion and solving the general diffusion equation to find the coefficient of diffusion and specific concentration equation through a computational software generated code. After importing the images into computational software and running analysis (**Figure 3**), the coefficient of diffusion can be assessed (**Table 2**). **Figure 4** represents the plots of the diffusion of rhodamine through the five tested collagen concentrations. The shapes of the diffusion plot match the traditional shape of a linear diffusion model. It can be seen that diffusion of rhodamine is inversely proportional to the concentration of collagen—the lower the collagen density the faster the diffusion. This is to be expected, as this concentration of collagen has a higher porosity. The horizontal lines in the collagen diffusion plot at a concentration of 1.5 mg/ml (**Figure 4B**) are simply the result of over saturation of the tracer signal. More importantly, as shown in **Figure 4** each line represents a specific point (x, y) inside the collagen, to whereas time increases the normalized concentration never exceeds the previous point at the same time (dt), indicating no reversal of the chemical. This is an important characteristic of a chemotaxis chamber to allow direct flow of a chemoattractant without reverse flow.

By examining the last ten images at each x location, one is able to generate a plot of the steady-state concentration of rhodamine at each of the locations. By extrapolating across the entire sample length (**Figure 5**), one can to look at the whole sample. This indicates that the linear diffusion gradient is consistent across the entire sample length, which can be utilized for cell experiments (**Figure 6**).

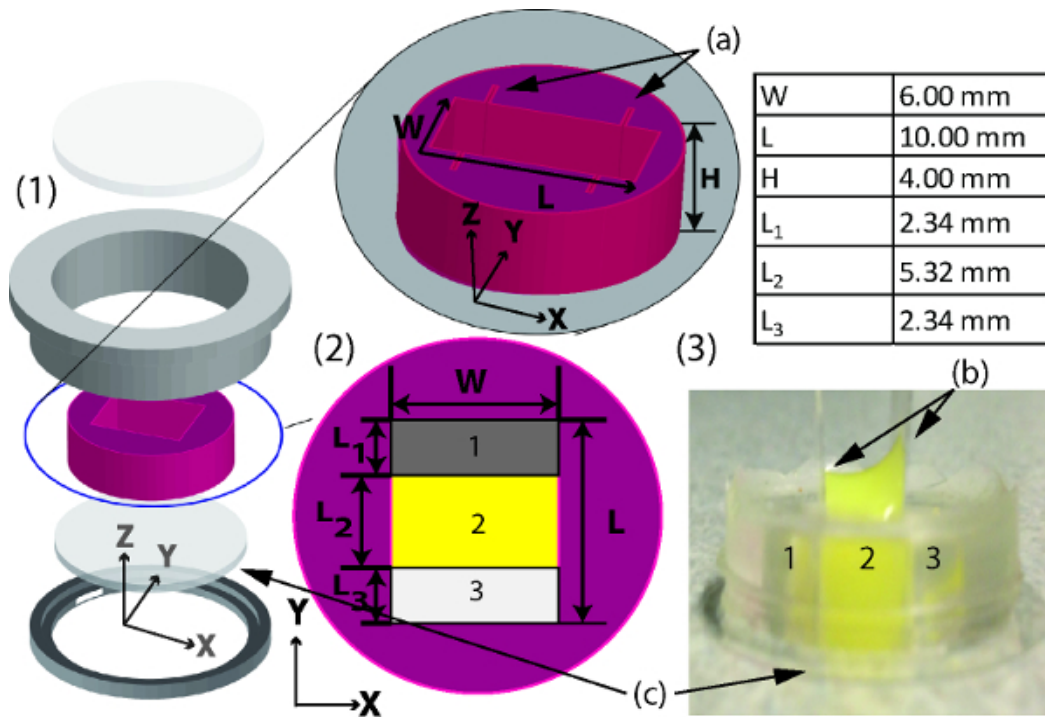


**Figure 1: A schematic of planar gradient diffusion system mold assembly in live cell imaging chamber.** (1) A computer rendition of the complete system consisting of (from bottom to top) a bottom housing (c) a hydrophilic 22 mm coverslip, mold, top housing, and a glass cover. (2) Dimensions of mold where (a) cut inserts are shown. (3) Mold with collagen matrix with (b) hydrophobic coverslips on each side slid into the cut inserts to create the 3-well system. [Please click here to view a larger version of this figure.](#)

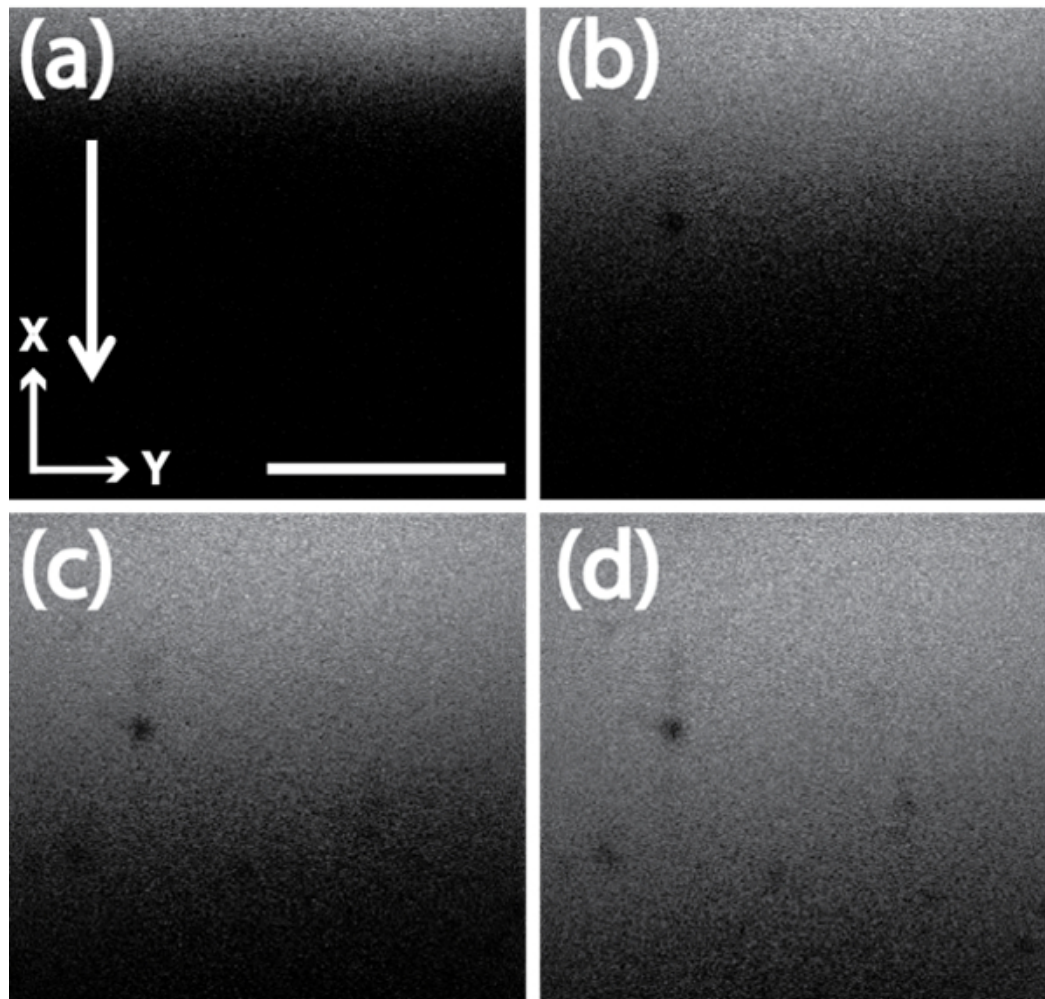


**Figure 2: Example of rhodamine microscopy images in collagen.** Representative images taken during rhodamine diffusion experiments, at same z-axis location, in the planar gradient diffusion system with a 1.0 mg/ml collagen concentration. Scale bar = 500  $\mu\text{m}$  where (a) is 0 min (b) 3 min (c) 7 min, and (d) 15 min after rhodamine was added to chamber. Arrow indicates direction of diffusion of rhodamine through the collagen matrix. [Please click here to view a larger version of this figure.](#)

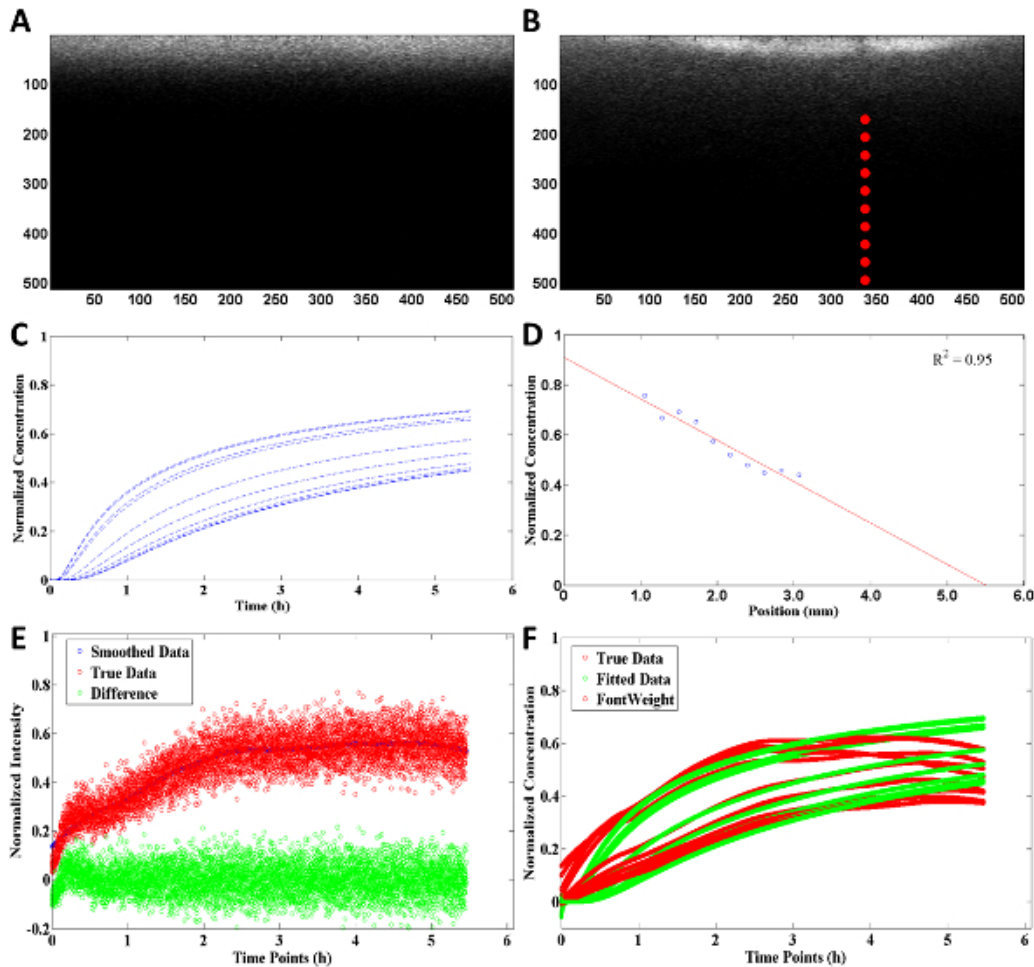


**Figure 3: Example of analysis and summary of diffusion calculations generated by computational software code with a 2.5 mg/ml collagen concentration.** (A) Black and white rendering of initial ( $dt = 0$ ) image uploaded into computational software for analysis. (B) Specific points chosen by the user for intensity comparison and for diffusion calculations (x, y-axis are in pixels). (C) Diffusion profile of rhodamine throughout the collagen matrix where each line correlates to a red point in image B. (D) Concentration profile of rhodamine throughout the collagen matrix at steady-state. (E) Comparison between the smoothed data (blue dot) and true data from diffusion experiment (red dot) with difference between smoothed and true (green dot). (F) Normalized concentration of true (red dot) and fitted (green dot) data from computational software code throughout the experiment. [Please click here to view a larger version of this figure.](#)

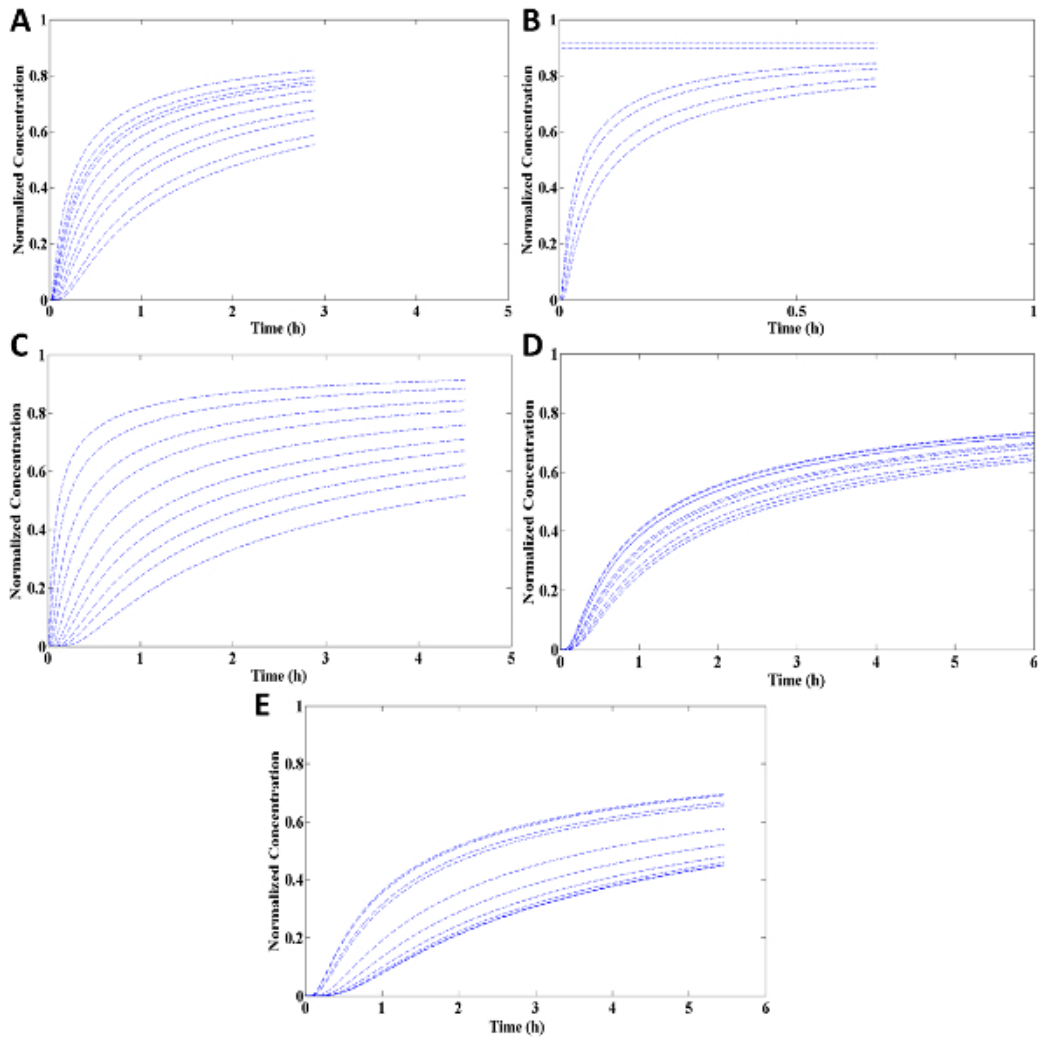


**Figure 4: Example of diffusion profile through collagen matrix using the planar gradient diffusion system at different points.** Each line indicates a different selected data points chosen from the computational software code by the user. Collagen matrix at a density of (A) 1.0 mg/ml (B) 1.5 mg/ml (C) 2.0 mg/ml (D) 2.2 mg/ml and (E) 2.5 mg/ml. [Please click here to view a larger version of this figure.](#)



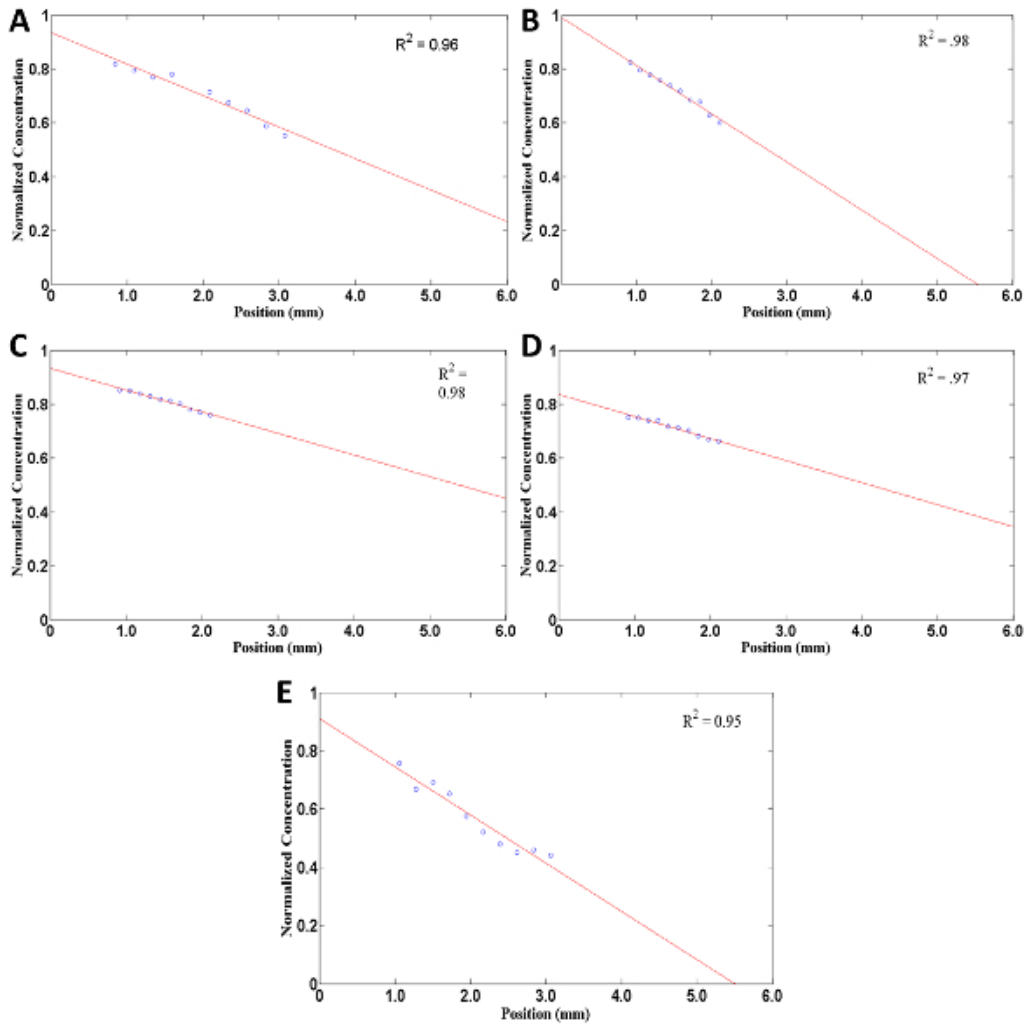


**Figure 5: Example of a concentration (normalized) profile of rhodamine throughout the collagen matrix using the planar gradient diffusion system at steady-state.** Circles are specific data points chosen through the computational software code by the user. Red line constructed using data points and extrapolating best line-fit (with  $R^2$  value shown) to show rhodamine concentration throughout the whole collagen matrix. Collagen matrix at a density of (A) 1.0 mg/ml (B) 1.5 mg/ml (C) 2.0 mg/ml (D) 2.2 mg/ml and (E) 2.5 mg/ml. [Please click here to view a larger version of this figure.](#)

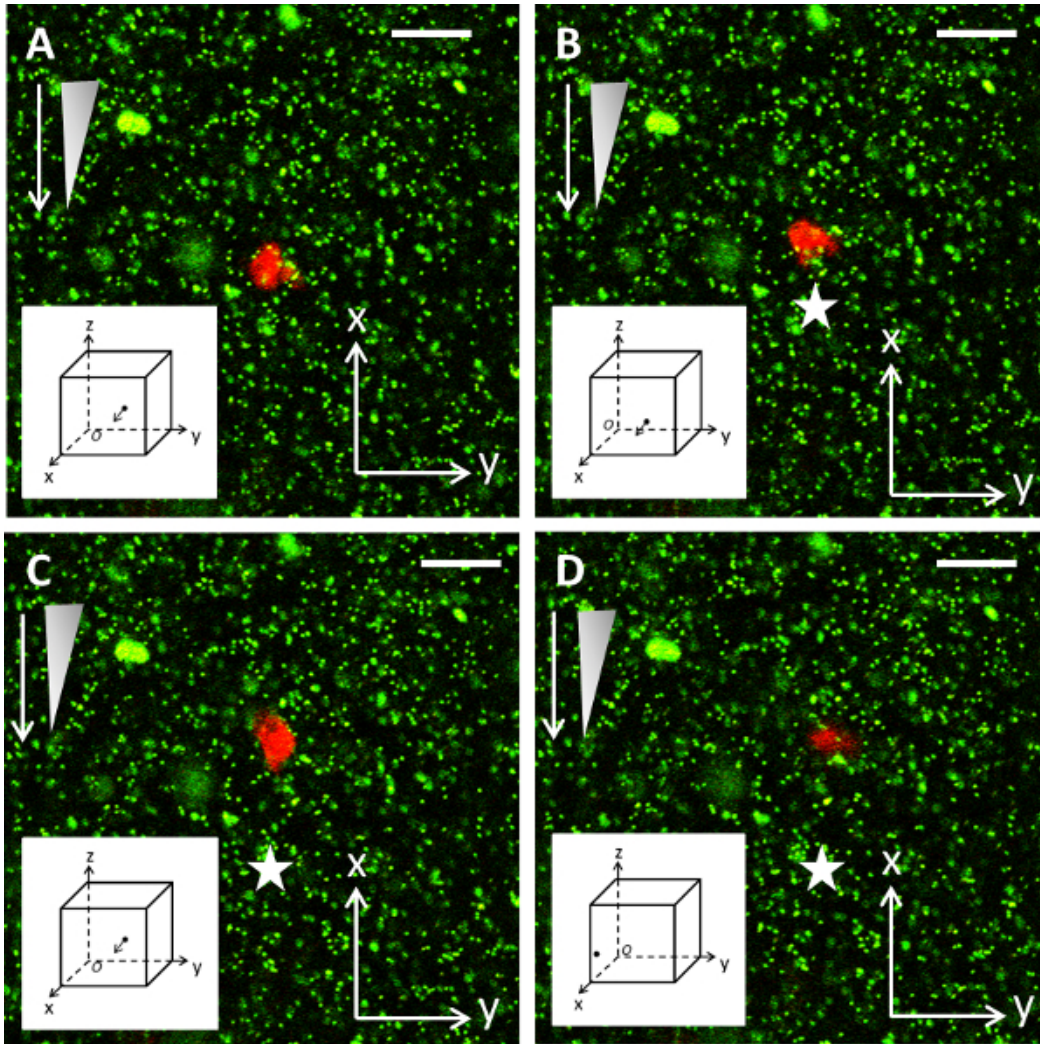


**Figure 6: Example of cell migration experiments.** A Z-slice microscope image of a neutrophil migrating in the 3D planar gradient system. Neutrophil migrates towards the chemoattractant gradient (white arrow depicts direction of gradient and the triangle shows its concentration profile), where the star indicates the initial position of the cell at the start of the experiment. Subplot shows cell in 3D space, where arrow indicates next time-point direction. Scale bar = 10  $\mu\text{m}$ .  $\text{dt} = 5$  min between images (*i.e.*, A-B). [Please click here to view a larger version of this figure.](#)

Collagen Cell Density	PBS	Fluorescent beads	NaOH	Collagen I Rat Tail	Media
2.5 mg/ml	10%	6%	2%	70.20%	11.80%
2.2 mg/ml	10%	6%	2%	61.70%	20.30%
2.0 mg/ml	10%	6%	2%	56.10%	25.90%
1.5 mg/ml	10%	6%	2%	42.10%	39.90%
1.0 mg/ml	10%	6%	2%	28.10%	53.90%

**Table 1: Custom collagen mixture adapted for the addition of fluorescent beads and cell viability.**

Concentration of collagen Gel	Coefficient of Diffusion (cm <sup>2</sup> /sec)
2.5 mg/ml	$1.03 \times 10^{-6} \pm 2.54 \times 10^{-7}$
2.2 mg/ml	$1.28 \times 10^{-6} \pm 3.53 \times 10^{-7}$
2.0 mg/ml	$6.48 \times 10^{-6} \pm 1.66 \times 10^{-7}$
1.5 mg/ml	$1.05 \times 10^{-5} \pm 2.04 \times 10^{-7}$
1.0 mg/ml	$1.39 \times 10^{-5} \pm 1.06 \times 10^{-7}$
Water	$1.50 \times 10^{-5}$

**Table 2: Coefficients of diffusion.**

## Discussion

The most critical steps for successful diffusion experiments with or without cells are: correctly setting up the mold assembly; developing the necessary manual dexterity to prevent damage during extraction of hydrophobic coverslips; ensuring to find a very good linear starting line to correctly calculate the diffusion coefficient; correct experimental calculations of both collagen and chemoattractant; correctly use of live cell imaging system to ensure matrix does not dry out; and maintaining a sterile, healthy culture.

When conducting diffusion experiments, it is imperative to make sure the diffusion plots match the traditional shapes of a linear diffusion model (**Figure 4**).

Running the analysis at several different x-locations on each sample, it is possible to calculate the average coefficients of diffusion for rhodamine in the various concentrations of collagens, as reported in **Table 2**. These results are consistent with previous research—coefficient of diffusion through the collagen gel decreases as the concentration of collagen decreased due to an increase of porosity in the matrix.

According to the diffusion model equation at steady state, one expects to have a linear concentration profile across the x values. By fitting a linear function to the points, one can see that they are all, in fact, linear. The R<sup>2</sup> value of fitting a linear trend line for each of the best fit lines for the three collagen concentrations were at or above 0.92. The norms of the residuals in all extrapolated plots were .0227, indicating a good fit. This linear relationship is in agreement with the analytical solution. The concentration does not begin at 100%, as would be expected, because the imaging does not begin directly at the edge of the collagen sample. It is also impossible to perfectly calibrate the imaging.

Additionally, we were able to reference other papers that looked at diffusion in gels to compare results. Shenoy and Rosenblatt found the diffusion coefficient of BSA (radius = 4 nm) in a 30 mg/ml succinylated collagen solution to be  $2.2 \times 10^{-7}$  cm<sup>2</sup>/sec<sup>32</sup>. The radius of rhodamine is 0.78 nm, which explains its faster diffusion time through collagen<sup>24</sup>. In diffusion studies, it is common to utilize the radius to compare molecules. As the radius increases, the molecular weight also increases. Ramanujan *et al.* found the diffusion coefficient of dextran (radius = 6 nm) in polymerized 20% collagen gels (equivalent of 2.0 mg/ml concentration gels) to be  $4.72 \times 10^{-8}$  cm<sup>2</sup>/sec<sup>24</sup>. Again, this is comparable to the diffusion coefficient we observed for the 2.0 mg/ml concentration gel ( $D = 1.28 \times 10^{-6}$  cm<sup>2</sup>/sec), if we take into account the molecule size difference. Leddy and Guilak studied the diffusion of dextrans through articular cartilage<sup>33</sup>. It is possible to compare diffusion through collagen matrices and through articular cartilage because approximately two-thirds of the mass of articular cartilage is polymeric collagen (predominately type II). Leddy and Guilak found the diffusion coefficient of 3 kDa dextran through articular cartilage to be between  $6-10 \times 10^{-7}$  cm<sup>2</sup>/sec<sup>33</sup>. Knowing that the system works properly we were then able to calculate the specific concentration anywhere within the system, using sawtooth and transient system heat transfer models. This additional metric can be used during cell experiments to track cell-concentration understanding and gradient slope.

Time duration of experiments may be a limiting factor when using our approach. Therefore, it is important to use a cover for the live cell imaging system to ensure the matrix does not dry out. Using a cover during experiments, we were able to successfully monitor the diffusion of rhodamine up to 7 hr and 4 hr during cell experiments without the gel drying up. If one does not use a cover, the gel might dry up faster and significantly affect the diffusion and migration of cells.

The protocol described herein uses a well-controlled planar diffusion model/system to be able to measure cell forces in a 3D environment during chemotaxis. Here we present a newly developed simple system that can be utilized for TFM/DVC experiments. Using this system, the researchers will be able to: 1) successfully model diffusion through 3D collagen matrices and verify, by fitting the data to analytical expression, that the planar gradient diffusion system, when seeded with cells, should promote chemotaxis and not chemokinesis; 2) calculate the coefficient of diffusion for collagen of five different concentrations; and 3) successfully find the specific concentration of the chemoattractant within the diffusion chamber. With this approaches, one can further examine cell chemotaxis with specific metrics not easily and readily available without the laborious approaches of multifaceted systems and complex diffusion gradients.

## Disclosures

The authors declare that they have no competing financial interests.

## Acknowledgements

The authors would like to acknowledge Drs. Jonathan Reichner and Angle Byrd for cell experiment insight. The National Science Foundation Graduate Research Fellowship Program (GRFP) supported this work.

## References

- Adzick, N. S. The Molecular and Cellular Biology of Wound Repair. *Ann Surg.* **225**, (2), 236 (1997).
- Reddi, A. H. Bone morphogenetic proteins: an unconventional approach to isolation of first mammalian morphogens. *Cytokine Growth F. R.* **8**, (1), 11-20 (1997).
- Coussens, L. M., Werb, Z. Inflammation and cancer. *Nature.* **420**, (6917), 860-867 (2002).
- Vital-Lopez, F. G., Armaou, A., Hutnik, M., Maranas, C. D. Modeling the effect of chemotaxis on glioblastoma tumor progression. *AIChE J.* **57**, (3), 778-792 (2011).
- Hughes-Alford, S. K., Lauffenburger, D. A. Quantitative analysis of gradient sensing: towards building predictive models of chemotaxis in cancer. *Curr. Opin. Cell Biol.* **24**, (2), 284-291 (2012).
- Friedl, P., Gilmour, D. Collective cell migration in morphogenesis, regeneration and cancer. *Nat. Rev. Mol Cell Bio.* **10**, (7), 445-457 (2009).
- Cristini, V. Morphologic Instability and Cancer Invasion. *Clin. Cancer Res.* **11**, (19), 6772-6779 (2005).
- Lammermann, T., et al. Rapid leukocyte migration by integrin-independent flowing and squeezing. *Nature.* **453**, (7191), 51-55 (2008).
- Parent, C. A., Devreotes, P. N. A cell's sense of direction. *Science.* **284**, (5415), 765-770 (1999).
- Boyden, S. The chemotactic effect of mixtures of antibody and antigen on polymorphonuclear leucocytes. *J. Exp. Med.* **115**, 453-466 (1962).
- Nelson, R. D., Quie, P. G., Simmons, R. L. Chemotaxis under agarose: a new and simple method for measuring chemotaxis and spontaneous migration of human polymorphonuclear leukocytes and monocytes. *J. Immunol.* **115**, (6), 1650-1656 (1975).
- Rosoff, W. J., McAllister, R., Esrick, M. A., Goodhill, G. J., Urbach, J. S. Generating controlled molecular gradients in 3D gels. *Biotechnol. Bioeng.* **91**, (6), 754-759 (2005).
- Wells, A., Kassis, J., Solava, J., Turner, T., Lauffenburger, D. A. Growth factor-induced cell motility in tumor invasion. *Acta Oncol.* **41**, (2), 124-130 (2002).
- Wilkinson, P. C. Assays of leukocyte locomotion and chemotaxis. *J. Immunol. Methods.* **216**, (1-2), 139-153 (1998).
- Bonvin, C., Overney, J., Shieh, A. C., Dixon, J. B., Swartz, M. A. A multichamber fluidic device for 3D cultures under interstitial flow with live imaging: development, characterization, and applications. *Biotechnol. Bioeng.* **105**, (5), 982-991 (2010).
- Noo, L. J., et al. Neutrophil chemotaxis in linear and complex gradients of interleukin-8 formed in a microfabricated device. *Nat. Biotechnol.* **20**, (8), 826-830 (2002).
- Shao, J., et al. Integrated microfluidic chip for endothelial cells culture and analysis exposed to a pulsatile and oscillatory shear stress. *Lab Chip.* **9**, (21), 3118-3125 (2009).
- Haessler, U., Kalinin, Y., Swartz, M. A., Wu, M. An agarose-based microfluidic platform with a gradient buffer for 3D chemotaxis studies. *Biomed. Microdevices.* **11**, (4), 827-835 (2009).
- Friedl, P., Wolf, K. Tumour-cell invasion and migration: diversity and escape mechanisms. *Nat. Rev. Cancer.* **3**, (5), 362-374 (2003).
- Sixt, M., Lammermann, T. In vitro analysis of chemotactic leukocyte migration in 3D environments. *Methods Mol. Biol.* **769**, 149-165 (2011).
- Zigmond, S. H. Ability of polymorphonuclear leukocytes to orient in gradients of chemotactic factors. *J. Cell Biol.* **75**, (2 Pt 1), 606-616 (1977).
- Zicha, D., Dunn, G. A., Brown, A. F. A new direct-viewing chemotaxis chamber. *J. Cell. Sci.* **99**, (Pt 4), 769-775 (1991).
- Gilbert, D. L. Macromolecular diffusion through collagen membranes. *Int. J. Pharm.* **47**, (1-3), 79-88 (1988).
- Ramanujan, S., et al. Diffusion and convection in collagen gels: implications for transport in the tumor interstitium. *Biophys. J.* **83**, (3), 1650-1660 (2002).
- Weadock, K., Silver, F. H., Wolff, D. Diffusivity of 125I-calmodulin through collagen membranes: effect of source concentration and membrane swelling ratio. *Biomaterials.* **7**, (4), 263-267 (1986).
- Erikson, A., Andersen, H. N., Naess, S. N., Sikorski, P., Davies, C. dL. Physical and chemical modifications of collagen gels: impact on diffusion. *Biopolymers.* **89**, (2), 135-143 (2008).
- Moghe, P. V., Nelson, R. D., Tranquillo, R. T. Cytokine-stimulated chemotaxis of human neutrophils in a 3-D conjoined fibrin gel assay. *J. Immunol. Methods.* **180**, (2), 193-211 (1995).
- Sundd, P., et al. Live cell imaging of paxillin in rolling neutrophils by dual-color quantitative dynamic footprinting. *Microcirculation.* **18**, (5), 361-372 (2011).
- Sanders, E. R. Aseptic Laboratory Techniques: Volume Transfers with Serological Pipettes and Micropipettors. *J. Vis. Exp.* (63), 2754 (2012).
- Stephenson, F. H. *Calculations for Molecular Biology and Biotechnology: A Guide to Mathematics in the Laboratory 2e.* Elsevier Science (2010).
- Bar-Kochba, E., Toyjanova, J., Andrews, E., Kim, K., Franck, C. A Fast Iterative Digital Volume Correlation Algorithm for Large Deformations. *Exp. Mech.* **In press** (2014).
- Shenoy, V., Rosenblatt, J. Diffusion of Macromolecules in Collagen and Hyaluronic Acid, Rigid-Rod-Flexible Polymer Composite Matrixes. *Macromolecules.* **28**, (26), 8751-8758 (1995).
- Leddy, H., Guilak, F. Site-Specific Molecular Diffusion in Articular Cartilage Measured using Fluorescence Recovery after Photobleaching. *Ann. Biomed. Eng.* **31**, (7), 753-760 (2003).